Journal of Ceramic Processing Research. Vol. 25, No. 5, pp. 827~841 (2024)
(Received 1 July 2024, Received in revised form 30 July 2024, Accepted 5 September 2024)
https://doi.org/10.36410/jcpr.2024.25.5.827

J O U R N A L O F
Ceramic Processing Research

Chromogenic mechanisms of overglaze red pigment produced in the Jingdezhen kiln during the Ming dynasty

Meng Hao[a], Maolin Zhang[a,*], Yanjun Weng[b,*] and Zhe Xiong[b]
[a]*School of Archaeology and Museology, Jingdezhen Ceramic University, Jingdezhen 333403, China*
[b]*Institute of Jingdezhen Imperial Kiln, Jingdezhen 333000, China*

To elucidate the compositions and chromogenic mechanisms of overglaze red pigment produced in the Jingdezhen kiln during the Ming dynasty, we employed energy-dispersive X-ray fluorescence spectrometry, Raman microspectroscopy, scanning electron microscopy, and single-factor simulations to analyse 16 specimens of overglaze pigment porcelain fired in the Jingdezhen kiln during the Ming dynasty. Results indicated that α-Fe_2O_3 crystals are the chromogenic agent in overglaze red pigments. However, the composition and crystallinity of the α-Fe_2O_3 crystals varied among specimens. Overglaze red pigment produced before the Chenghua era had a low Fe_2O_3 content and mostly exhibited a bright red hue, whereas those produced from the Chenghua era onwards had more diverse compositions and appeared bright red or dark red. The overglaze red pigment produced during the Jiajing era had high Fe_2O_3 and PbO content and were generally found to have a deep red hue. Simulation experiments indicated that increasing the calcination temperature of $FeSO_4·7H_2O$ results in greater disruption of the long-range order of α-Fe_2O_3 crystals, thereby producing deeper hues of red. The results of the study will be of great significance for the conservation and identification of overglaze red pigment porcelain in the Jingdezhen kiln.

Keywords: Jingdezhen kiln, Overglaze red pigment, Chemical composition, Phase structure, Chromogenic mechanism.

Introduction

Ancient China has a long history of using red glaze. Although the red pigment used Fe_2O_3 for colouring, the raw materials varied significantly. During the Late Neolithic period, painted pottery surfaces used red pigments made from materials such as ochre [1], which consists of hematite, without the addition of any other materials in the kiln. From the Song (960-1279 CE) Dynasty, there have only been two types of low-temperature overglaze red pigments: the iron-based red pigment and the gold-based red pigment. The gold-based red pigment was developed in Western, and introduced to China during the Kangxi period. Beforehand, the overglaze red pigments in Chinese ceramics were only iron-based red pigment. The earliest use of iron-based red pigment was seen in the Jin (1115-1234 CE) Dynasty at the Shanxi Changzhi Dongshan kilns, Hebei Magnetic Kiln, and other northern kilns; the pigment was produced using alum ($FeSO_4·7H_2O$) as the raw material, which was calcined, crushed, and so on, then mixed with lead powder [2]. From a historical perspective, the technology of overglaze red pigment was developed during the Song and Jin Dynasties. During the Yuan (1279-1368 CE) and Ming (1368-1644 CE) dynasties, Jingdezhen kiln fully inherited and progressed this technology, creating various overglaze porcelains and marking the beginning of the decorative porcelain era in Chinese ceramic history. Red pigment became the primary colour of overglaze decoration, used either alone, as a base for gold decoration, or applied to DouCai and WuCai porcelain. The introduction of overglaze red pigment was necessary for the development of overglaze decorations, significantly influencing the history of Chinese porcelain.

Literature indicates that the invention of iron-based red pigment is closely related to the widespread use of alum during the Song and Jin Dynasties. In the Northern Song Dynasty, alum was a government monopoly [3]. The History of the Song Dynasty records: “Green alum from Ci, Xi State(慈、隰州), and Tongling County in Chizhou, was collected by officials, and wok households sold it to the official market." Xizhou, now called Shanxi Linfen Xi County (山西临汾隰县), was an important source of green alum [4]. Su Song of the Northern Song recorded in "Tu Jing Ben Cao": "There are five kinds of Alum, white alum(白矾), green alum (绿、青矾), yellow alum(黄矾), black alum(黑矾), and Jiang Alum(绛矾). White alum is used in medicine and dyeing; green alum is also used in throat and mouth medicine as well as colouring; yellow alum is used in Dan home stoves, and is also used in medicine. Black alum, found only in Xirong, is called soap alum and is used for dyeing sideburns and in medicine. Jiang

*Corresponding author:
Tel : 15079895581
Fax: +86-798-8490226
E-mail: zhangmaolin@jci.edu.cn (Maolin Zhang)
yanjun_weng@yeah.net (Yanjun Weng)

alum, originally green, also known as the stone gall (石胆), is burned to red colour, hence the name Jiang, which is rarely available." [5] "Compendium of Materia Medica" contains the following: "Green alum, which red colour known as jiang alum. Shizhen stated that green alum can dye soaps, so it is called soap alum. Black alum is also known as soap alum and is not suitable for human consumption, but is used as a natural remedy for sores. The red variety is commonly known as alum, to distinguish it from Zhu Hong. An ode mentions that green alum was discovered Hot Springs County in Xizhou, and Tongling County in Chizhou, by frying alum. Initially, it appears as stone and is decocted; its original appearance resembles that of nitrate and is green. When heated on an iron plate with charcoal, the boiling alum produced a rich red colour like that of golden liquid. Once this red liquid was exhausted, the colour would like Yellow Dan(黄丹). There are also types of alum called "soap Fu alum", which refer to green alum. Green alum found in grottoes was not exposed to air and therefore had the appearance of glass, leading people to think it was stone gall(石胆). Burning to red colour, so the name of the jiang alum. Out of Guazhou good. Shizhen said that green alum was sourced from Jindi, Henei, Xi'an, and Shazhou, and had the shape of flame nitrate (焰硝). Among them, the one who picks out the deep green glittering and clean is the green alum; if it turns red, it is the jiang alum. Green alum was mostly used by plasterers and painters, but the carriers also used sand and soil as blocks. Historically, green alum was confused with stone gall(石胆) [6]. The Song Huiyao Series Draft mentions that over 11300 pounds of green, gall, and yellow alum was decocted from Lead Mountain fields in Xinzhou [7]. In the Song Dynasty, green alum had wide-ranging applications such as medicine, alchemy, dyes, and lacquerware. When calcined and dehydrated, green alum hydrolyzed to α-Fe_2O_3, known as raw red (or Jiang alum). This natural iron pigment was also historically used in grotto paintings, such as the Mogao Grottoes five generations of 005 grottoes, the Song Dynasty 378 grottoes, Yuan 465 grottoes, etc. [8, 9]. The red pigment of all these grotto paintings was from the red pigment from jiang alum; it did not contain quartz and was highly pure, achieving the same colour as the iron red pigment used nowadays. These historical records show that the kiln workers fully mastered the characteristics of alum in the Song Dynasty. Thus,the iron-based red pigment was indeed invented by ancient Chinese craftsmen and was first used to decorate porcelain [10].

In nature, the iron-based natural mineral pigments vary widely, with Fe_2O_3 contents ranging from 12% to 90%. Most of these pigments are composed of iron oxide-containing chromogenic phases and clay mineral-type non-chromogenic phases, all of which are chemically stable. From the perspective of the history of ceramic technology, alum can be successfully used as a red pigment primarily because of two characteristics: wide availability and high iron oxide content (up to 95% after calcination), making it ideal for dyeing and coating performance [11]; therefore, it is suitable for the production requirements of overglaze red pigment. Overglaze red pigment has remained a topic of immense interest among researchers for decades, it can be broadly categorised into three areas – study of its composition, techniques, and chromogenic mechanism. In research on composition, Pamela Vandiver, Anne Bouquillon, and others conducted Proton Induced X-ray Emission (PIXE) quantitative analysis on overglaze pigments from the three periods of Jin, Yuan, and Ming; they discussed the chromogenic agents used in overglaze pigments [12]. Xiong et al. suggested that the changes in the composition and proportions of lead and chromogenic materials in red pigments influenced the hue of pigments [13]. Wu et al. compared the characteristics of overglaze red pigment from the Yuan, Ming, and Qing dynasties, and concluded that the ancient deep-red pigments used in Jingdezhen were using Fe_2O_3, whereas the purplish-red hue of the gold-based red pigment that emerged during the Kangxi era was due to gold nanoparticles (colloids) in the metallic state [14]. By comparing the Doucai porcelain of the Ming dynasty and the famille rose porcelain of the Qing dynasty, Zhao et al. determined that Fe was the chromogenic element of the red pigments of the Ming and Qing Dynasties, whereas Hg was the chromogenic element of deep-red pigments [15]. Ye et al. further pointed out that the pigment formulas for overglaze red pigment in Jingdezhen's famille rose porcelain were relatively similar before the Republic of China period, but underwent significant changes afterwards [16]. In research on production techniques involved in overglaze red pigment, Zhang et al. first reported that $FeSO_4 \cdot 7H_2O$ was the raw material of overglaze red pigment. Ferric oxide powder was first produced through a series of processes, including heating, calcination, fine grinding, and drying, and the decoration of porcelain objects was achieved by the low-temperature firing of a mixture of ferric oxide powder, lead oxide powder, and cowhide glue in appropriate proportions [17]. Two studies [18, 19] independently demonstrated the characteristics of overglaze red pigment through archaeological excavation data and simulation studies, which included the evaluation of the opaqueness, low firing temperature, high susceptibility to detachment, and high tendency to be overlaid by other pigments. Zhao et al. investigated Doucai specimens from the Ming dynasty with optical microscope (OM) and swept-source optical coherence tomography (OCT) and reported that the Doucai was extremely meticulous and intricate. The specimens consisted of several layers, with the overglaze pigments mostly used for infilling, patching, and embellishment [20]. Kajihara et al. found that when the calcination temperature of alum reaches 650 °C, iron sulfate transforms into α-Fe_2O_3 [21]; Li et al. noted that at 650 °C, $Fe_2(SO_4)_3$ and α-Fe_2O_3 coexist, and

at 700 °C, $Fe_2(SO_4)_3$ desulfurizes to produce α-Fe_2O_3, the colour is beginning to change [22]; Hashimoto et al. pointed out that when the calcination temperature of alum exceeds 700 °C, the particle size of α-Fe_2O_3 increases, and the quantity decreases with increasing temperature [23]. Jun-Il Song et al. discussed the effects of milling speed on the structural evolution of Fe_2O_3 agglomerates in terms of the crystallite size and surface area [24]. In research on the chromogenic mechanisms involved in overglaze red pigment, Chen et al. determined that hematite is the chromogenic agent in the red pigments of the Ming dynasty [25]. In another study, Wang et al. determined that Fe^{3+} is the chromogenic species in red pigments via X-ray absorption fine-structure (XAFS) spectroscopy [26] and identified three main factors related to colouration in red pigments based on structural analysis [27]. Colomban et al. pointed out that the narrow characteristic peaks in the Raman spectrum indicated that the composition of hematite was very close to that of α-Fe_2O_3 [28]. J. Van Pevenage et al. further proved that the overglaze red pigment was colored by α-Fe_2O_3 in ancient Chinese porcelain [29]. Hidika and his team, utilizing synchrotron radiation X-ray diffraction and X-ray absorption spectroscopy, discovered that the coloration of the overglaze red pigment is mainly induced by micro-structural correlation between α-Fe_2O_3 fine particles of red-pigment emission element and the oxide complexes of SiO_2-Al_2O_3-CaO-KNaO or SiO_2 in the fritted overglazes [30]. Using a combination of Raman spectroscopy and X-ray diffraction (XRD) techniques, Hao et al. demonstrated that the crystal structure of α-Fe_2O_3 in overglaze red pigment decoration was distorted to different degrees [31]. Pan and her team innovatively utilized the capillary focused microbeam X-ray fluorescence spectrometer, and the capillary focused X-ray diffraction spectrometer to indicate that the Fe mineral crystal phases in the raw materials for the overglaze red pigment may disappeare during the firing process, and the Fe_2O_3 crystal phases have been left or generated during the process of firing or cooling [32]; de Lucas et al. noted that the hematite tended to turn greyish-brown during firing, making it a technical and economic challenge to achieve a vivid overglaze red pigment [33].

Despite a multitude of analytical studies on overglaze pigments, certain aspects have not been explored comprehensively because of the preciousness and rarity of overglaze red pigment specimens. These include the evolutionary patterns of the composition of overglaze red pigment produced in Jingdezhen during the Ming dynasty; the relationship between colouration and the crystal structure of the chromogenic agent, that is, α-Fe_2O_3; and the influence of the calcination of $FeSO_4 \cdot 7H_2O$ on the colouration of overglaze red pigment. In this context, we utilized energy-dispersive X-ray fluorescence spectrometry, raman spectroscopy, and scanning electron microscopy for a comparative analysis of the chemical compositions and phase structures of overglaze red pigment in differently coloured ceramic specimens produced in Jingdezhen kiln during the Ming dynasty. Subsequently, we simulated the firing conditions based on the molecular formulas of red pigments documented in ancient texts. By varying the calcination temperature of the raw materials and the firing temperature of the

Table 1. Appearances of the specimens analysed in this study.

Serial No.	Specimen No.	Era	Decoration style	Site unearthed	Appearance/characteristics
a	MXD-1	Xuande	Qinghua Hongcai	Jingdezhen, Jiangxi Province	Thick, heavy white porcelain body. The exterior surface of the fragment was decorated with motifs and branches outlined with a blue pigment and infilled with overglaze red pigment. The red pigment was detached from a large area of the porcelain due to wear and tear.
b	MXD-2	Xuande	Doucai	Jingdezhen, Jiangxi Province	Thin, lightweight white porcelain body. White glaze on the exterior surface of the fragment was decorated with lotus motifs using red pigment. The motifs were outlined with an intense red pigment and shaded with a pale red one, indicating the adoption of an intricate drawing method that created a clear layering effect.
c	MCH-1	Chenghua	Honglücai	Jingdezhen, Jiangxi Province	White porcelain body. The exterior surface of the fragment contained an iron-based red pigment as the base, on which Lingzhi motifs were drawn in a green pigment.
d	MCH-2	Chenghua	Honglücai	Jingdezhen, Jiangxi Province	White porcelain body. The exterior surface of the fragment contained an iron-based red pigment as the base, on which Lingzhi motifs were drawn in a green pigment. A large area of the red pigment had detached.
e	MCH-3	Chenghua	Honglücai	Jingdezhen, Jiangxi Province	White porcelain body decorated with curly grass motifs in an iron-based red pigment. The red pigment exhibited a dark red hue.

Table 1. Continued.

Serial No.	Specimen No.	Era	Decoration style	Site unearthed	Appearance/characteristics
f	MCH-4	Chenghua	Honglücai	Jingdezhen, Jiangxi Province	White porcelain body decorated with curly grass motifs in an iron-based red pigment. The red pigment exhibited a dark red hue.
g	MCH-5	Chenghua	Doucai	Jingdezhen, Jiangxi Province	Thin, lightweight, and fine-textured white porcelain body. Embellishments on the exterior surface of the fragment were outlined with blue underglaze. Flowers were infilled with overglaze red decoration, whereas leaves were drawn with green overglaze.
h	MCH-6	Chenghua	Doucai	Jingdezhen, Jiangxi Province	Thin, lightweight, and fine-textured white porcelain body. Outlines were drawn with blue underglaze, and dragon motifs were drawn with red, green, and yellow overglazes.
i	MCH-7	Chenghua	Doucai	Jingdezhen, Jiangxi Province	Thin, lightweight, and fine-textured white porcelain body. Outlines were drawn with blue underglaze, and floral motifs were drawn with red, green, and yellow overglazes.
j	MZD-1	Zhengde	Doucai	Jingdezhen, Jiangxi Province	Thin, light, and fine-textured white porcelain body. The exterior surface of the fragment was decorated with red and green overglazes.
k	MZD-2	Zhengde	Qinghua Hongcai	Jingdezhen, Jiangxi Province	Fine-textured white porcelain body. The white glaze on the fragment surface was decorated with dragon motifs drawn in blue underglaze and infilled with overglaze red pigment.
l	MJJ-1	Jiajing	Honglücai	Jingdezhen, Jiangxi Province	The exterior surface of the fragment was decorated with intertwined branch and floral motifs, drawn in overglaze red pigment, and infilled with green overglaze. Both the red and green pigments were extensively corroded and peeled.
m	MJJ-2	Jiajing	Honglücai	Jingdezhen, Jiangxi Province	The exterior surface of the fragment contained a green pigment as the base, on which floral motifs were drawn in a red pigment. Both the red and green pigments were extensively corroded.
n	MJJ-3	Jiajing	Honglücai	Jingdezhen, Jiangxi Province	The exterior surface of the fragment was decorated with lotus petal motifs outlined with a red pigment and infilled with a green pigment. The pigments were severely degraded by soil corrosion.
o	MJJ-4	Jiajing	Honglücai	Jingdezhen, Jiangxi Province	The exterior surface of the fragment was decorated with intertwined branch and floral motifs outlined with overglaze red pigment and infilled with a green pigment. Certain areas of the red and green pigments were corroded or detached.
p	MJJ-5	Jiajing	Qinghua Hongcai	Jingdezhen, Jiangxi Province	The interior and exterior surfaces of the fragments were decorated with motifs outlined in a blue pigment and infilled with overglaze red pigment.

red pigments, we evaluated the colouration effect and crystallinity of α-Fe_2O_3 in the pigments. This analysis enabled us to explore the development of overglaze red pigment during the Ming dynasty. This study fully reflects the history of the development of overglaze pigment production technology and establishes its experimental and theoretical basis so as to comprehensively understand China's contributions to ceramic science and technology.

Experimental Section

Experimental specimens

A total of 16 overglaze red pigment specimens from the Xuande to Jiajing eras of the Ming dynasty were selected for investigation. All specimens were procured from the Jingdezhen Imperial Kiln Museum and were classified according to the era and decoration style. The specimens included one blue-and-white porcelain with red pigment fragment and one Doucaifragment from the Xuande era; four Honglücai (red and green) fragments and three Doucai fragments from the Chenghua era; one Doucai fragment and one blue-and-white porcelain with red pigment fragment from the Zhengde era; and four Honglücai fragments and one blue-and-white porcelain with red pigment fragment from the Jiajing era. A comparison of the hues of specimens from different eras

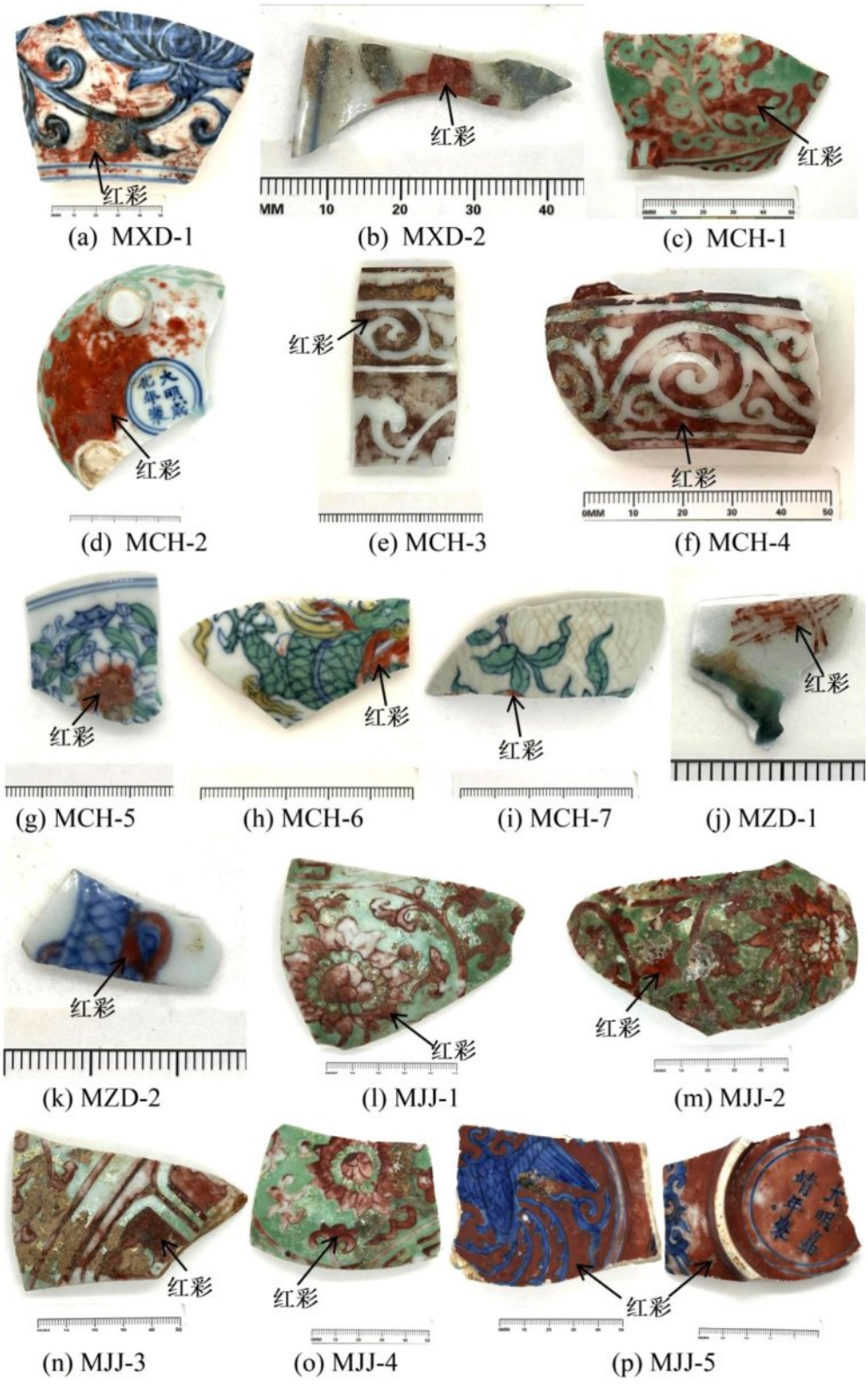

Fig. 1. Photographs of the porcelain specimens.

revealed that red pigments from the Xuande era were slightly darker than those from the Chenghua era. The specimens from the Chenghua era had greater variety and exhibited bright-red and dark-red hues, the red pigments from the Zhengde era were more vibrant, and a deep-red hue was found for most of the red pigments from the Jiajing era. In general, overglaze red pigment produced in Jingdezhen during the Ming dynasty could be classified as bright red, deep red, dark red and so on. Table 1 describes the appearances of the specimens

used in this study, and Fig. 1 presents the photographs of these specimens.

Testing and analytical methods

ED-XRF spectrometry

Specimens were cleaned in a CQ-250 ultrasonic cleaner for 20 min and dried in a 101-1 electric forced-air drying oven. Subsequently, the elemental compositions of the overglaze red pigment decoration from the Ming dynasty were determined using an EAGLE III XXL XRF spectrometer (EDAX Inc., USA) using the following parameters: X-ray tube pressure of 50 kV, tube current of 200 μA, beam path in vacuum, and an incident X-ray beam spot diameter of 300 μm. Each location on the sample was tested in triplicate, and semi-quantitative analysis was conducted with the built-in standardless fundamental parameter method. There are two reasons for semi-quantitative analysis: one is that the nature and state of the sample and its surface vary significantly: the glaze belongs to the low-temperature lead glaze system; the specimen contains high lead content, giving a high error that affects the other trace elements when deconvoluting the spectrum, especially in the low-energy region; and the quantitative analysis of the elemental composition is more difficult to carry out, mainly in the high-energy region of the measured spectrograms. Secondly, the amount of laser stripping when using ED-XRF to detect the composition of the glaze colour is large; the high-energy x-ray photons are able to penetrate relatively deeply (tens of micrometres) into the material, depending on the energy of the x-ray beam and absorption coefficients of the components of the analyte [34]; the colour layer of the glaze is generally thin; and the results of the measurement will be affected by the underglaze composition. Therefore, the collected photons may come from both the overglaze layer and the underlying high-temperature glaze, resulting in a relatively high content of Si and Al and a relatively low content of Pb. Additionally, when calculating the elemental composition of a sample using an online calculator for XRF signals, the software automatically selects the line used to quantify the content, usually the K line; however, when considering Pb, which is used on the surface of the overglaze, the L line must be selected for quantification. As the standards on which the analyses were based were consistent, the variability in the results of the data used did not affect the comparative study of the strengths of the elemental signals of the glazes, following a rigorous evaluation of the relevant XRF data.

Raman spectroscopy

The Raman equipment was a Renishaw in Via confocal Raman microscope. A 532-nm laser was chosen as the excitation source for the study, because overglaze pigments may undergo serious thermal changes when exposed to high-intensity radiation [35]. The equipment is fitted with a Laica microscope from Germany, an advanced feedback-controlled ultra-high-precision diffraction-grating turntable, and patented continuous scanning technology. The output power of the test was 50 mW and the power of the sample level was 0.2 mW to avoid heating the samples, and the laser beam was focused perpendicularly to the sample surface with a 50X objective lens; the spatial resolution was 0.5 μm in the horizontal direction and 2 μm in the vertical direction. The acquisition time for each spectrum was approximately 60 s, and the spectrum was recorded over the range of 50-2000 $cm^{-1,}$ with a spectral resolution of 1 cm^{-1}. The instrument was calibrated using single-crystal Si specimens prior to testing, and for each coloured region in the object, a minimum of three Raman spectra were recorded to ensure representative data. The data was processed with Origin 2022 software.

Scanning electron microscopy (SEM)

The SU-8010 Field Emission Scanning Electron Microscope (Hitachi, Ltd., Japan) was equipped with the Model 550i electro-cooled Energy-dispersive Spectrometer (EDS; IXRF, US), with the area of the electron beam spot at a minimum of 1-2 microns. Before the test, the glaze colour sample was cut into small pieces of approximately 5 mm × 5 mm × 5 mm and sprayed with platinum using a Quorum SC7620 sputtering coater for 45 s, then sprayed with gold at 10 mA. The accelerating voltage was approximately 0.1-30 kV. The resolution was 1.0 nm at an accelerating voltage of 15 kV and WD=4 mm or 1.3 nm at an accelerating voltage of 1 kV and WD=1.5 mm. The magnification was 25×; that of the secondary electron image was 800000×. The grain size in the overglaze red pigment decoration was calculated with the Nano Measurer software using the average of ten randomly selected grains.

Chromaticity analysis

A Japanese NIPPON DENSHOKU NF-333 portable

Table 2. Experimental instrumentation and parameters.

Instrument	Model number	Parameters
Constant temperature heater	HEATING PLATE-250	Temperature range: 0-100 ℃
Electronic balance	FA1004B	Maximum weight: 100 g
Planetary Ball Mill	DECO-PBM-V-0.4L	Maximum speed: 1100 r/min
Electrothermal blast thermostat box	XMTA-7000	Temperature range: 50-300 ℃
Ultra-High-Temperature Muffle Furnace	SGM-M36-17A	Maximum working temperature: 3000 ℃

spectrophotometer was used with a spectral range of approximately 400-700 nm, a spectral interval of 20 nm, and an output of 20 nm. All measurements were carried out under the standard 10° observation conditions using a D65 light source. In the L*a*b* colour space formulated by the International Commission on Illumination (CIE), L* represents the brightness of the sample surface, with values ranging from 0-100, 0 being the darkest and 100 being the brightest; a* represents the red-green value of the sample, with +a* indicating red and -a* indicating green; and b* represents the yellow-blue value of the sample, with +b* indicating yellow and -b* indicating blue. To ensure the accuracy of the results, an average of five measurements of each sample of the glaze was used, thus quantifying the small differences between the colours.

Simulation experiments

Industrial $FeSO_4 \cdot 7H_2O$ with a purity >99% and lead oxide powder. The single-factor experimental method was employed for the design of experimental processes to investigate the relationships between the calcination and firing temperatures of the red pigments and the changes in the lattice structure of the α-Fe_2O_3 crystals so as to establish a correlation between the results of the simulation experiments and the Ming Dynasty overglaze pigments. The experiments were carried out at the Research Centre for Ancient Ceramics, Jingdezhen Ceramic University, and the instrumentation and parameters used for the experiments are listed in Table 2.

Experiment 1: $FeSO_4 \cdot 7H_2O$ was first heated to 100 °C in a crucible to remove its waters of crystallization. It was then ground to approx. 200 μm to obtain a fine powder. The powder was calcined in a muffle furnace at 700, 750, 800, or 850 °C for 10 min at a temperature rise of 3 °C/min. Following the ball milling for 20 min, the sample was dried in a constant-temperature oven for 12 h, ground, and sieved. The resultant ultrafine Fe_2O_3 particles were mixed with lead oxide powder at a weight ratio of 1:5. Frankincense oil was added; the sample was mixed well and painted on a white porcelain plate at a uniform thickness. The decorated samples were fired in a muffle furnace at approximately 800 °C to obtain the final product.

Experiment 2: The crystal water of $FeSO_4 \cdot 7H_2O$ was removed by heating to 100 °C in a crucible. Then, the anhydrous $FeSO_4$ sample was ground to a powder with a particle diameter of approximately 200 μm and subsequently calcined in a muffle furnace at 700 °C for 10 min. Following calcination, the sample was ball-milled for 20 min, dried in a constant-temperature oven for 12 h, ground, and sieved. The resultant ultrafine Fe_2O_3 particles were mixed with lead oxide powder at a 1:5 weight ratio. Frankincense oil was added; the sample was mixed well and painted on a white porcelain plate at a uniform thickness. The decorated sample was fired in a muffle furnace at 700, 750, 800, or 850 °C for 10 min at a temperature rise of 3 °C/min to obtain the final product.

Results and Discussion

Elemental composition analysis

Table 3 presents the ED-XRF spectral data of overglaze red pigment specimens unearthed from the site of the Jingdezhen imperial kiln of the Ming dynasty. The samples were found to be composed primarily of

Table 3. Semi-quantitative analysis results of ED-XRF spectrometry performed on overglaze red pigment produced in Jingdezhen during the Ming dynasty (wt%).

Specimen No.	Na_2O	MgO	Al_2O_3	SiO_2	P_2O_5	K_2O	CaO	TiO_2	MnO	Fe_2O_3	PbO
MXD-1	3.11	0.36	10.26	65.89	2.88	2.03	5.52	0.09	0.2	6.1	3.55
MXD-2	1.13	1.17	10.43	67.15	5.52	2.52	3.17	0.07	0.1	4.55	4.21
MCH-1	3.33	0.45	12.18	61.18	0.31	1.84	2.73	0.13	0.15	7.98	9.71
MCH-2	1.75	0	10.35	65.41	0.86	1.67	2.94	0.1	0.19	7.96	9.78
MCH-3	4.03	0.13	8.72	54.53	0.34	1.37	2	0.1	0.08	7.83	20.87
MCH-4	3.59	0.25	11.86	47.51	0.34	1.61	1.46	0.18	0.04	10.3	22.87
MCH-5	2.84	0.29	10.72	68.12	0.33	3.1	3.45	0.1	0.09	4.61	6.36
MCH-6	2.99	0.21	11.37	70.07	0.56	4.64	4.62	0.1	0.11	2.95	2.39
MCH-7	2.86	0.3	10.41	71.12	0.57	3.82	4.19	0.11	0.1	2.97	3.55
MZD-1	2.95	0.39	9.14	69.99	0.33	2.08	4.15	0.07	0.1	5.06	5.74
MZD-2	3.49	0.31	9.92	70.04	0.5	3.81	5.3	0.06	0.11	4.61	1.45
MJJ-1	2.57	0.39	10.03	59.92	1.15	1.52	3.66	0.07	0.12	8.13	12.43
MJJ-2	3.94	0.34	9.65	57.53	0.98	1.76	4.84	0.11	0.16	10.95	9.75
MJJ-4	3.32	0.4	9.96	53.14	0.65	1.04	4.73	0.09	0.12	11.94	14.59
MJJ-5	3.03	0.35	9.54	50.59	1.31	1.83	4.03	0.14	0.14	17.89	11.16

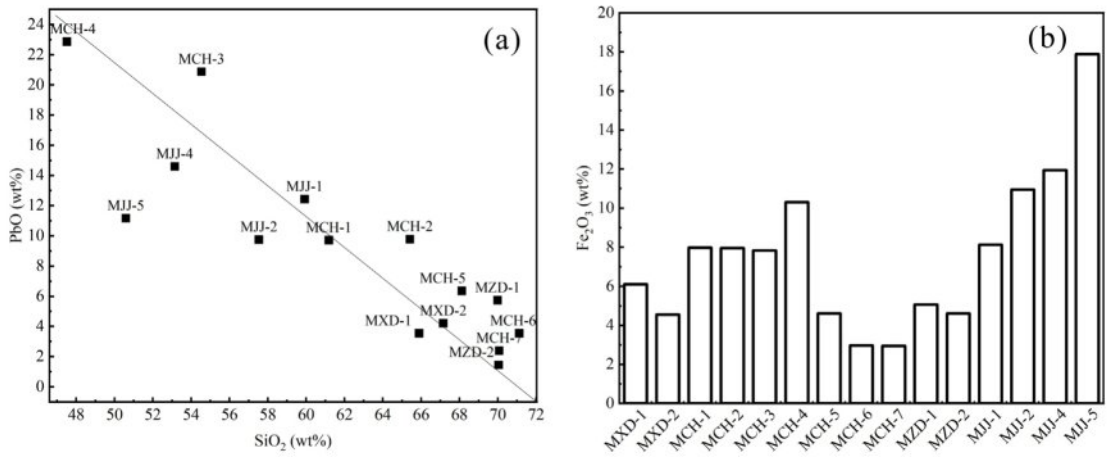

Fig. 2. (a) Scatter plot of the changes in the SiO_2 and PbO contents of overglaze red pigment, (b) Bar diagram of the Fe_2O_3 content.

SiO_2 and PbO, with their contents being in the ranges of 47-72 and 1.4-23 wt%, respectively. The scatter plot of the Si and Pb contents in Fig. 2a reveals a negative correlation of the SiO_2 content with that of PbO. PbO is known to act as a flux in red pigments, reducing the melting temperature of the pigment and allowing better adhesion of the chromogenic agent (Fe_2O_3 particles) to the glaze surface. The ED-XRF results suggest that the red pigments produced before the Chenghua era generally had a low PbO content. From the Chenghua era onwards, the amount of PbO added to pigments was varied, and low- and high-lead pigments were produced. The PbO content in pigments remained high during the Jiajing era, which was manifested as high-lead overglaze pigments.

Fe_2O_3 serves as the chromogenic material in red pigments. Fig. 2b illustrates a bar diagram of the Fe_2O_3 contents of specimens with a overglaze red pigment. Evidently, red pigments produced before the Chenghua era had a low Fe_2O_3 content. Conspicuous changes were found in the Fe_2O_3 content of red pigments produced in the Chenghua era, with the lowest and highest Fe_2O_3 content being found in Doucai and Honglücai porcelain specimens, respectively. Red pigments produced during the Jiajing era had a significantly higher Fe_2O_3 content than those produced in the previous eras.

MnO and TiO_2 present in red pigments also have certain chromogenic effects. However, the effects of these oxides in overglaze red pigment can be neglected, because their contents were found to be less than 1 wt% in overglaze red pigment.

In general, red pigments produced before the Chenghua era had relatively low Fe_2O_3 and PbO contents and exhibited mostly a bright red hue. From the Chenghua era, overglaze red pigment had more diverse compositions and could be broadly classified into two types: (i) low-lead, low-iron bright overglaze red pigment and (ii) high-lead, high-iron deep or dark overglaze red pigment. The overglaze pigments produced during the Jiajing era had high Fe_2O_3 and PbO contents and generally exhibited a deep red hue. Thus, Fe_2O_3 and PbO contents are the key factors that influence the colouration of overglaze red pigment.

Compositional analysis showed that before the Chenghua period, the production of overglaze red pigment at the imperial kilns in Jingdezhen during the Ming Dynasty was in its initial stage, and and there was only one formula for the overglaze red pigment. The Ming History [36] mentioned that in the third year of Hongwu, the public service court dress was changed to red, influenced by the social climate of the time. Consequently, there was a strong pursuit of red decoration in porcelain production. However, the firing requirements for underglaze red decoration were extremely stringent, that is, the colour was extremely sensitive to the contents of colouring oxides as well as to the firing temperature and atmosphere, making it considerably difficult to achieve a pure colour. In this context, the stable, bright, and pure overglaze red pigment came into being and was introduced into the Jingdezhen kilns, becoming increasingly popular. According to archaeological findings, the production of overglaze red pigment during the Hongwu, Yongle, and Xuande dynasties built upon the technological advancements of the previous dynasty, showing innovation and steady development. Notably, The remnants of a bowl with the Doucai pattern produced by the Xuande dynasty have been excavated [37], confirming the significant breakthrough in overglaze pigment technology made in the Xuande period, greatly contributing to the development of overglaze pigment-related technologies. During the Zhengtong, Jingtai, and Tianshun dynasties, the court frequently implemented policies to ban the burning firing of porcelain in kilns, stopping the production of overglaze pigment porcelain. Volume 161 of "Ming Shilu - Yingzong Shilu" recorded the following: “In the 12th year of Zhengtong, on the 11th day of December, the Jiangxi Rao state government forbade

the private production of yellow, purple, red, green, green, blue, white blue, white, and other porcelains" [38]. This explains the low production of overglaze red pigment in Jingdezhen during this period. In the Chenghua period, the Imperial Ware Factory resumed the production of overglaze red pigments having various distinctive features. Sun characterised it as "bright red, the colour as bright as blood, with uneven thickness; oil red, with dark and light shades" [39]. The advancement of the overglaze red pigment indirectly promoted the development of Doucai. Gongshi in the Jingdezhen pottery song: "white tire burned on the color red to come, five colors into the kiln paintings open. All kinds of fay flowers and figures, Longmian from the bottle to earthenware" [40]. Zhu's "Pottery Said" notes the following: "The paintings of colour vary, and the painters are different. All the colours of the ware must be out of the fire and then set. With the mixing, the formulas and amounts shall be precise. The colour must be very fine and even, allowing the colour to permeate the porcelain and display its full hue. Ancient porcelain with Wucai, Chenghua kiln for the most, its point of view vivid, out of the Danqing family above. Painter solid high, painting material is also fine ..... " [41]. During the Ming dynasty, the Jingdezhen imperial factory of the Chenghua dynasty produced the finest overglaze pigment porcelains. The pigments were characterized as uniform, well-coloured, vivid, and evocative. Because of the intricate colouring process, the Doucai porcelain was very expensive in this period. Zhang in the "Night Boat" wrote the following: "Into the kiln Daming Chenghua years made. There are Wucai chicken jar, light blue flower Zhu ware tea ou wine cup, all enjoy high price" [42]. "Pottery Said" also recorded the following: "Ancient porcelain with Wucai, Chenghua kiln for the most, wine cup to the chicken tank for the most, Shenzong fashion food before the Imperial, into a pair of cups, worth money 100,000" [43]. In addition, overglaze decoration technology has also undergone significant changes during this period; the richness of the overglaze pigment significantly enhanced the expressive power of the designs. By the Chenghua period, the flat paint technique began to be used. During the Hongzhi and Zhengde periods, the production of overglaze red pigment did not increase greatly, which is closely related to the state of porcelain production in Jingdezhen. Volume 45 of "Ming Shilu - Xiaozong Shilu" recorded the following: "Hongzhi three years in November A Chen ..... burned porcelain within the official stops not bad, is also one of the end of the repair province to eliminate the disaster! " [44]

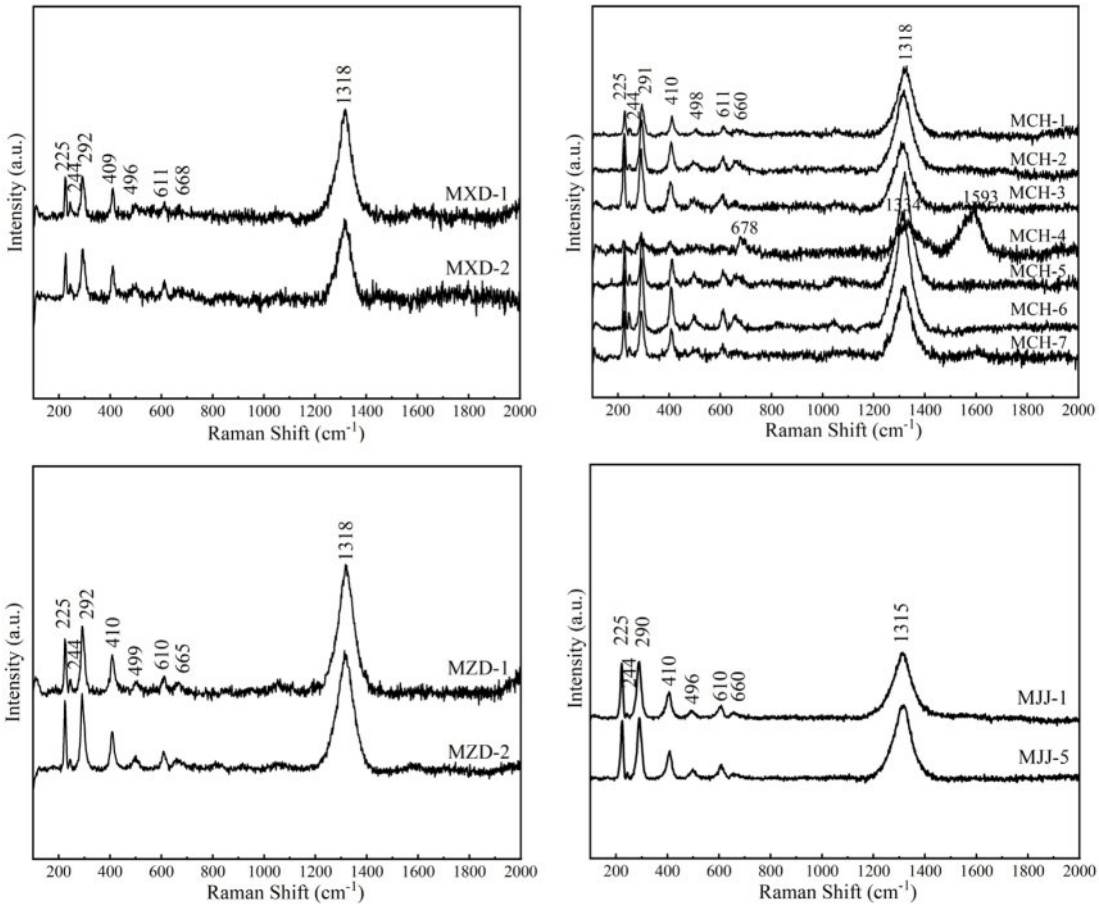

Fig. 3. Raman spectra of overglaze red pigment from the Ming dynasty (λ = 532 nm).

Volume 61 recorded the following: "mica porcelain altar, high head Luan, white list, white Kans, alum red ..... and other items, since Hongzhi two years before the December delinquency of the uncollected, all with the remission." [45]. Volume 143 recorded the following: "Jiangxi burned all kinds of magnetic ware, are extremely obscene ... Vol hope a comply with the old system, very amount, all stop; not suitable to stop, the responsibility of the period into the Na; the severance of the officer, the passage to retrieve, the people can be wide" [46]. During the Zhengde period, porcelain production made good use of overglaze red and green pigments. Overglaze red pigment was seen as gorgeous and was often used to accentuate patterns. The "red pigment painted on yellow pigment" became more popular, meaning "Hongfuqitian". After the Jiajing period, the expansion of the porcelain export market and the emergence of "the government produces porcelain in tandem with the people" system led to significant development of porcelain production in Jingdezhen. Improvements in the composition of the overglaze red pigment greatly increased the varieties of colours. Particularly, the production of Wucai was very successful for a while. Da Ming Canon recorded the following: “In the second year of the Jiajing period, porcelain made in Jiangxi changed from bright underglaze red decoration to deep iron-based overglaze red pigment” [47]. Huang noted in "Things Cyanote": "Jiajing kiln’s finest blue-and-white porcelain, bright red soil cut off, the production technique is not as good as before, can burn iron-based roverglaze red pigment only" [48]. This implies that the use of overglaze red pigments became more prominent. Jingdezhen's ceramic production focused on rich reds and greens, creating vibrant and colorful designs that met the royal requirements for 'dragon and phoenix' and 'flowers and grasses,' resulting in elaborate and beautiful ceramics.” [49] However, by the late Ming period, issues such as ruling corruption, economic recession, and intensified social conflicts declined the production of Jingdezhen overglaze pigment porcelains. Conversely, folk kilns owing to the development of the market economy, leading them to surpass the official kilns in production quality.

Relationship between the phase structure and colouration of overglaze red pigment

Figure 3 presents the Raman spectra and characteristic Raman peak positions for overglaze red pigment produced in Jingdezhen during the Ming dynasty. Except for the MCH-4 (see Table 1) specimens, which lacked individual characteristic peaks, all other overglaze red pigment specimens exhibited a series of characteristic Raman peaks with different intensities at approximately 225, 244, 291, 410, 498, and 611 cm^{-1} and a high-intensity characteristic peak at 1318 cm^{-1}, which typically corresponds to the bimagnon effect [50]. Previous reports have attributed these Raman peaks to the characteristic vibrations of hematite (α-Fe_2O_3), based on the spectral library [51, 52]. According to group theory, the optical vibrational modes of α-Fe_2O_3 belong to the D_{3d}^6 point group and consist of seven Raman-active vibrational modes: two A_{1g} modes (225 and 497 cm^{-1}) and five E_g modes (244, 291, 299, 410, and 612 cm^{-1}). The chromogenic agents in overglaze red pigment in Jingdezhen during the Ming dynasty were derived mainly from hematite [53]. In the Raman spectra of the overglaze red pigment of MXD-2 and MCH-3f specimens, certain characteristic signals were broadened or did not appear. Researchers have suggested that this may be related to the increased disorder of α-Fe_2O_3 in the red pigment or the masking of Raman signals [54].

In addition to these characteristic Raman peaks of hematite, a clear Raman peak was observed at approximately 660 cm^{-1} in the spectra of certain overglaze red pigment specimens. The appearance of this peak can be attributed to (i) the presence of magnetite (Fe_3O_4), which imparts a dark red hue to the red colour in the overglaze red pigment [55] and (ii) the disruption of the long-range order of α-Fe_2O_3 crystals. This disruption can be attributed to two main causes, the first being lattice distortion in the primary crystals, which affects the Raman selection rules. The second main cause of the disruption of the long-range order of α-Fe_2O_3 is its decreased grain size. When the grain size of α-Fe_2O_3

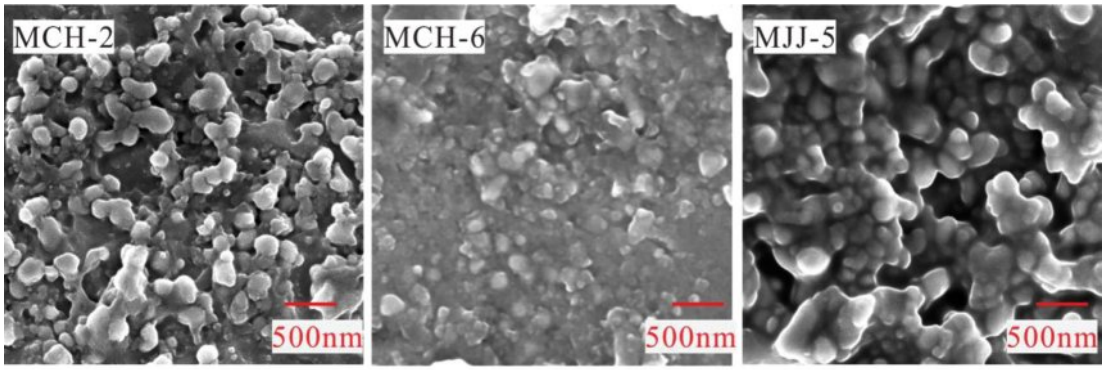

Fig. 4. Back-scattered electron microscopy images of overglaze red pigment.

is reduced to the nanometre scale, changes are induced in the long-range translational symmetry, which causes frequency shift and broadening of Raman peaks [56].

However, the possibility of recrystallisation of Fe_2O_3 into spinel Fe_3O_4 under the action of the laser is largely ruled out at illumination powers below 0.5 mW [57]. In addition, the Raman spectra of the overglaze red pigment did not reveal the characteristic peaks of magnetite at other positions, such as 297 cm^{-1} and 535 cm^{-1} [58]. The chemical reduction of Fe_2O_3 to Fe_3O_4 requires high-temperature firing in a reducing atmosphere, which is in complete contrast to the firing mechanisms of overglaze red pigment. Therefore, the characteristic peak at 665 cm^{-1} is unlikely to be due to magnetite; instead, it may be related to the long-range order of α-Fe_2O_3 crystals. Our subsequent investigation was thus focused on the grain size and lattice distortion of the Fe_2O_3 crystals.

First, the grain size of certain specimens was measured through SEM analysis. Considering the value of the specimens and the destructive nature of the SEM sample preparation process, we selected three representative specimens for SEM analyses. The grain sizes of MCH-2, MCH-6, and MJJ-5 were measured multiple times, and the average values are 185, 133, and 196 nm, respectively (Fig. 4). Evidently, the grain sizes of the overglaze red pigment decoration produced in Jingdezhen during the Ming dynasty were greater than 100 nm, which far exceeds 8 nm and had virtually no effect on the shift in the characteristic Raman peaks [59]. Therefore, the characteristic peak at 665 cm^{-1} is deduced to be related primarily to lattice distortion. The disruption of the long-range order of α-Fe_2O_3 crystals in overglaze red pigment produced in Jingdezhen during the Ming dynasty was caused mainly by the distortion of the crystal structure of hematite.

The crystallinity of a material can be characterized by analysing its characteristic Raman peaks. A high degree of crystallinity usually leads to narrower Raman peaks, whereas the disruption of the crystal lattice or low crystallinity causes the broadening of the Raman peaks. In the Raman spectra of silicates containing alkali and alkaline earth metal species, the peaks in the 800-1200 cm^{-1} range represent the symmetric stretching vibrations of non-bridging oxygen atoms in $Si\text{-}O_{nb}$ [60]. Those peaks in the 400-800 cm^{-1} range are attributed to the bending vibrations of the bridging oxygen atoms (Si–O–Si) in silicon-oxygen tetrahedra, whereas the peaks at 400 cm^{-1} or below correspond to metal–oxygen vibrations and lattice vibrations, which reflect the long-range order of the crystals in the silicate structure [61]. The structure of natural hematite is non-stoichiometric. In the Raman spectra, the pure α-Fe_2O_3 phase exhibits an extremely narrow hematite peak, which changes with heat treatment or partial substitution of iron by Al or Ti, etc., leading to broadening of the hematite Raman peaks (in particular, in the 290 cm^{-1} band, which can be characterised as an oscillatory mode that is very sensitive to the degree of structural disorder) and changes in the intensity (with the wave number 225-290 cm^{-1} doublet dominating) [62]. Therefore, the full-width at half-maximum (FWHM) of the Raman peak at 290 cm^{-1} was used to characterize the long-range order of α-Fe_2O_3 crystals. Table 4 shows the FWHM values of the glaze specimens from various eras examined in this study. The Raman spectra and 290 cm^{-1} full width at half-maximum (FWHM) calculations of all the Ming glazed red-coloured specimens and the simulated experimental samples below were processed under the same conditions. Due to the subtraction of the baseline using the Origin software, the calculated values of FWHM may be slightly biased [63]. However, the FWHM values here are not used as absolute data, but only as comparative data, and are therefore meaningful. The FWHM of the Raman peak at 290 cm^{-1} of deep red pigment was significantly larger than that of bright red pigment decoration. This result indicates that the long-range order of the α-Fe_2O_3 crystals in deep red pigment was disrupted to a greater extent and the deeper-hued red pigment had a higher degree of crystal distortion.

Table 4. FWHM values of the Raman peak at 290 cm^{-1} of overglaze red pigment from various eras of the Ming dynasty.

Specimen No.	FWHM
MXD-1	18.8
MXD-2	17.75
MCH-1	20.64
MCH-2	20.13
MCH-3	26.7
MCH-4	33.43
MCH-5	17.07
MCH-6	17.58
MCH-7	17.71
MZD-1	19.31
MZD-2	18.62
MJJ-1	22.06
MJJ-5	29.7

Relationship between the preparation process and colouration of red pigments used in overglaze red pigment decoration

The long-range order of α-Fe_2O_3 crystals in overglaze red pigment of the Ming dynasty is associated mainly with lattice distortion. However, the craftsmen of this era would not have known the concept of the long-range order of α-Fe_2O_3 crystals; they controlled the colouration effects by altering the preparation processes of overglaze red pigments. Overglaze red pigment use alum as raw material, followed by dehydration, high-temperature calcination to generate α-Fe_2O_3 particles, and adding lead oxide as a flux in Jingdezhen Kiln. The analysis of the samples demonstrates that when using alum as raw material for the production of overglaze red pigment,

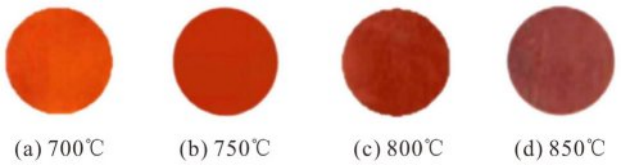

Fig. 5. Photographs of iron-based overglaze red pigment specimens obtained at different calcination temperatures.

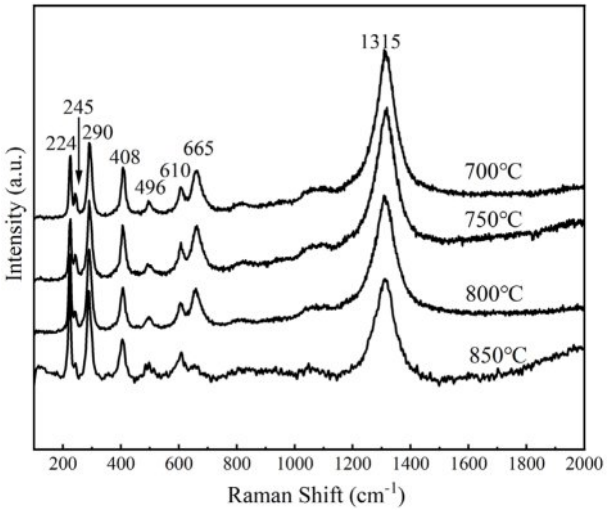

Fig. 6. Raman spectra of overglaze red pigment specimens.

the hue is affected by several factors, including the proportion of lead powder, the calcination temperature, hematite crystal size, the thickness of the glaze, and the temperature of its firing. However, the greatest influence on the colour is the degree of lattice distortion of the α-Fe_2O_3 crystals. Several scholars suggest that if the α-Fe_2O_3 crystal lattice structure is altered by ion doping (Al or Ti), heat treatment, or other factors, the D_{3d}^6 point group symmetry will appear broken [64, 65]. Several scholars also pointed out that the α-Fe_2O_3 crystal lattice distortion deformation is the most pronounced when the alum is calcined at a temperature high enough to generate ferric oxide powder [66]. Due to the Fe_2O_3 content of up to 99% or so produced by alum calcining, the influence of ionic doping is small. However, scholars have proved that, when the alum calcination temperature reaches 700 °C, the overglaze red pigment can exists in the form of the α-Fe_2O_3 crystal state completely [67]. Combining with the Raman spectra of the overglaze red pigment samples, we conclude that all samples are coloured with α-Fe_2O_3 crystals. Consequently, the calcination temperature of the Ming Dynasty overglaze red pigment should be above 700 °C. Therefore, in this study, while maintaining the same experimental conditions of raw material formula, fineness of the powder, and thickness of colour decoration. Two sets of simulation experiments were designed to explore the relationship between the changes in the crystal-lattice structure of α-Fe_2O_3 crystals and the firing temperatures, both for the calcination of alum and the colour firing of theover glaze red decoration, so as to establish the correlation between the simulation experimental results and the colour on glazes of the Ming Dynasty.

Figure 5 shows the overglaze red pigment specimens produced under different calcination temperatures. First,

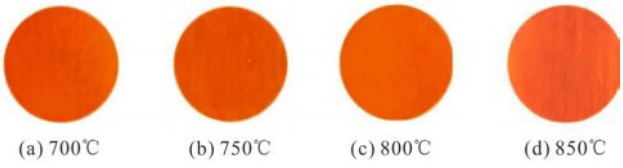

Fig. 7. Photographs of overglaze red pigment specimens obtained with different colour-baking temperatures.

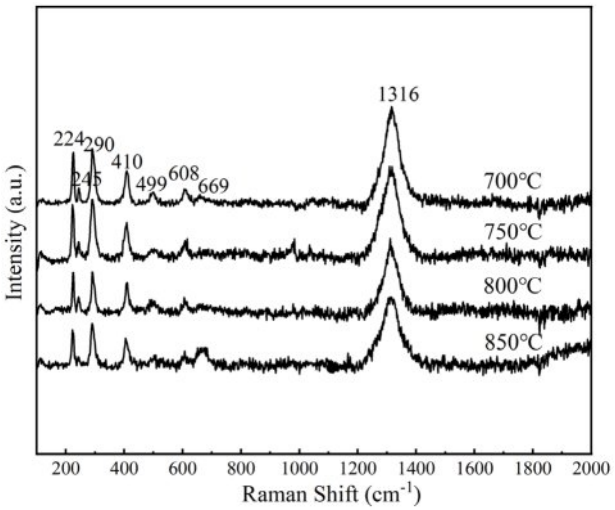

Fig. 8. Raman spectra of overglaze red pigment specimens obtained with different colour-baking temperatures.

Table 5. FWHM values of the Raman peak at 290 cm^{-1} of overglaze red pigment specimens obtained at different calcination temperatures.

Calcination temperature	FWHM	L*	a*	b*	Colouration
700 °C	17.8	45.45	41.92	49.09	Orange red
750 °C	19.23	42.05	40.06	31.53	Bright red
800 °C	21.15	34.92	38.55	26.48	Deep red
850 °C	25.8	28.68	30.99	18.22	Dark red

Table 6. FWHM values of the Raman peak at 290 cm^{-1} of overglaze red pigment specimens obtained with different colour-baking temperatures.

Colour-baking temperature	FWHM	L*	a*	b*	Colouration
700 °C	17.69	52.82	31.75	28.4	Orange red
750 °C	17.99	48.75	33.24	28.73	Orange red
800 °C	17.82	48.79	33.47	37.37	Orange red
850 °C	17.62	49.32	38.38	49.28	Orange red

the specimens were examined by Raman spectroscopy. Figure 6 shows the obtained Raman spectra, and Table 5 lists the experimentally measured L*, a*, and b* values of the samples and the full width at half peak (FWHM) of the Raman peak at 290 cm^{-1} obtained by fitting with Origin software. For the samples of overglaze red pigment prepared under the same conditions, when the calcination temperature of alum reaches 700 °C, with an increase of the calcination temperature, the half-peak full width at 290 cm^{-1} (FWHM) of the corresponding Raman spectra gradually increases, and the degree of disorder of the α-Fe_2O_3 crystal structure becomes larger. Simultaneously, the L*, a*, and b* values of the samples are negatively correlated with the alum calcination temperature, and the colouration of the red pigment exhibited a change of orange-red → bright red → deep red → dark red, indicating that the hue of the red pigment deepened with an increase in the degree of the lattice distortion of the α-Fe_2O_3 crystals.

Next, the alum calcined at 700 °C was used to prepare overglaze red pigment specimens via decoration colour-baking at different temperatures. Figures 7 and 8 show the obtained specimens and the corresponding Raman spectra, respectively, and Table 6 lists the FWHM values of the Raman peak at 290 cm^{-1} and the L*, a*, and b* values of the various specimens. The results demonstrate that, for the samples of overglaze red pigment prepared under the same conditions, the full width of the half peak (FWHM) of the 290 cm^{-1} band is basically unaffected by the colour-baking temperature within a certain range of temperatures, that is, the destruction of the crystal structure of α-Fe_2O_3 is basically unrelated to the colour-baking temperature. All samples show the colours of the α-Fe_2O_3 particles after the colour materials have been calcined.

The findings described above demonstrate that the difference in the calcination temperature of alum is one of the important factors affecting the colour rendering of overglaze red pigment, which is manifested mainly in the change in the disorder of the α-Fe_2O_3 crystal structure. The characteristics of the specimens revealed that the overglaze red pigment from the Ming dynasty exhibited various red hues, such as bright red, deep red, and dark red. Therefore, it can be deduced that the raw materials of overglaze red pigment produced in Jingdezhen during the Ming dynasty were generally calcined at 700 °C and above. An increase in the calcination temperature of alum led to a greater degree of disruption in the long-range order of α-Fe_2O_3 crystals and gradual deepening of the hue of red pigments.

Conclusion

Microscopic detection techniques, such as ED-XRF spectrometry and Raman micro-spectroscopy, were adopted to elucidate the composition and chromogenic mechanisms of overglaze red pigment on porcelain wares unearthed from the site of the Jingdezhen kiln of the Ming dynasty. Simulation experiments were subsequently performed to investigate the change patterns of the crystallinity of α-Fe_2O_3 grains in red pigments versus the calcination temperature of alum, that is, $FeSO_4 \cdot 7H_2O$. Results indicated that overglaze red pigment used in Jingdezhen kiln during the Ming Dynasty was based on SiO_2 and PbO, and the chromogenic element was Fe_2O_3. Before the Chenghua era, overglaze red pigments were mostly bright red in colour and had low Fe_2O_3 and PbO contents, and the temperature used to calcine alum to produce the ferric oxide powder was approximately 750 °C. From the Chenghua era onwards, overglaze red pigment had more diverse compositions and could be broadly classified into bright red and dark red. Among the bright red pigment specimens, the Doucai fragment from the Chenghua era had the brightest hue, with the temperature of the alum calcination being lower than 750 °C. Overglaze red pigment of the Zhengde era had a slightly darker hue and were possibly calcined at a slightly higher temperature of 750 °C. The Fe_2O_3 and PbO contents of dark red pigment were significantly higher, and the calcination temperature of the alum was above 850 °C. Red pigments produced during the Jiajing era contained high Fe_2O_3 and PbO contents and generally exhibited a deep red hue, suggesting that the calcination temperature of alum was approximately 800 °C. Composition analysis showed that the overglaze red pigment contained PbO, which had poor chemical stability, the lower hardness and it was easy to be scratched by hard objects. However, the colorant Fe_2O_3 was high, most of them were insoluble in the glaze. Overglaze red pigment was colored in the form of α-Fe_2O_3 crystals, and the crystals were suspended on the surface of the lead glaze in a granular state, with

poor adhesion and self-bonding ability. At the same time, the overglaze red pigment can present bright red, dark red, deep red, depends on the production technique. Based on this analysis, it can be seen that the overglaze red pigment is most likely to suffer from colour fading. Therefore, the protection and restoration of overglaze red pigment porcelain should focus on preserving and displaying the original pigment and colour. First, according to the relevant research, a comprehensive record card should be established for the overglaze red pigment used in the Jingdezhen kiln during the Ming dynasty. Then, cleaning, reinforcement and repair work must be undertaken. Throughout this process, the aim is to retain the original pigment and colour as much as possible. The combined use of traditional restoration techniques and modern scientific methods will ensure an effective approach to the restoration and protection of these cultural relics. In addition, the storage environment should be exceptionally controlled in terms of temperature, humidity, lighting conditions, and fireproofing.

Overglaze red pigment is formulated by mixing colourants with flux, with PbO being the primary flux. PbO is the main factor affecting the decorative quality of overglaze red pigment, greatly influencing the presentation of the colourant. To meet the continuously evolving standards of lead and cadmium dissolution limits in ceramic products [68] and align with the concept of green ceramics, it is also important to address the challenges of the traditional overglaze red pigment, which have poor colour rendering and stability. To effectively protect and preserve excellent traditional porcelain, it is necessary to ensure red colourants are pure and stable. This requires the continuous innovation and development of new ceramic materials, to reduce or replace lead and other harmful elements in the frit. By addressing these issues, we can fundamentally overcome the drawbacks of the traditional overglaze red pigment. This will broaden the market for overglaze red pigment porcelain, both domestically and internationally, and align with the trend of green ceramic decorative materials.

Acknowledgement

This research was financially supported by National Social Science Foundation of China (22VJXG025).

References

1. G. Li, Y. Guo, in "Technological Bases of Famous Chinese Porcelains" (Shanghai Science and Technology Press, 1988) p. 43.
2. Z. Wang, in "Jiangxi Dazhi- Volume 7" (Zhonghua shuju, 2018) p. 815.
3. T. Yuan, in "The History of the Song Dynasty- Volume 162, Officials II" (Zhonghua shuju, 2000) p. 2608.
4. T. Yuan, in "The History of the Song Dynasty- Volume 86, Geography II" (Zhonghua shuju, 2000) p. 1467.
5. S. Song, in "Tu Jing Ben Cao" (Anhui Science and Technology Press, 1994) p. 1061.
6. S. Li, in "The Compendium of Materia Medica" (People's Medical Press, 2010) p. 310.
7. S. Xu, in "Song Hui Yao Ji Gao" (Zhonghua shuju, 1957) p. 5399.
8. L. Xu, G. Zhou, in Proceedings of Dunhuang Research Anthology- Cave Conservation Volume, June 1993, edited by Dunhuang Academy (Gansu Nationalities Press, 1993) p. 187-197.
9. G. Zhou, in Proceedings of China Dunhuang Studies Centennial Library- Cave Conservation Volume, 1999, edited by Dunhuang Academy (Gansu Culture Press, 1999) p. 61-68.
10. J. Jiang, in Proceedings of Academic Seminar on Chinese Red and Green Color Porcelain, July 2011, edited by X. Guo (Cultural Relics Press, 2011) p. 53-68.
11. F. Zhang, in Proceedings of Ancient Chinese Scientific and Technological Achievements, December 1985, edited by J. Li, X. Chen, F. Zhang, Y. Guo and S. Chen (Shanghai Science and Technology Press, 1985) p. 338.
12. V. Pamela, B. Anne, K. Rose et al., in Proceedings of the 3rd International Symposium on Ancient Ceramics (ISAC'99), edited by J. Guo (Shanghai: Shanghai Science and Technology Literature Press, 1999) p. 218-227.
13. Y. Xiong, Y. Gong, and J. Wu, in Proceedings of the 9rd International Symposium on Ancient Ceramics (ISAC'15), edited by Y. Liu (Shanghai: Shanghai Science and Technology Literature Press, 2015) p. 92-95.
14. J. Wu, M. Zhang, and J. Wu, Spectrosc. Spect. Anal. 35[5] (2015) 1266-1270.
15. L. Zhao, Q. Li, J. Dong, S. Liu, and J. Jiang, Sciences of Conservation and Archaeology. 30[5] (2018) 98-109.
16. Z. Ye, M. Zhang, J. Wu, W. Lin, C. Hong, Y. Chen, and C. Cao, Sciences of Conservation and Archaeology. 30[5] (2008) 27-32.
17. F. Zhang, in Proceedings of the 3rd International Symposium on Ancient Ceramics (ISAC'99), edited by J. Guo (Shanghai: Shanghai Science and Technology Literature Press, 1999) p. 190-193.
18. X. Jiang, Palace Museum Journal. 02 (2016) 44-53.
19. J. Jiang, J. National Museum of China. 01 (2006) 46-57.
20. L. Zhao, Q. Li, J. Dong, S. Liu, and J. Jiang, Sciences of Conservation and Archaeology. 30[5] (2018) 98-109.
21. S. Kajihara, M. Hidaka, R. Wijesundera, L. Kumara, M. Koga, S. Kobayashi, T. Tsuru, K. Koga, K. Shimomura, J. Choi, et al., Ceram. Int. 34[7] (2008) 1681-1689.
22. Q. Li, A. Wu, M. Zhang, J. Li, J. Cao, H. Li, and Y. Jiang, Materials. 17 (2024) 2800.
23. H. Hashimoto, D. Kawabe, A. Terasawa, H. Inada, T. Takaishi, and T. Okura, J. Eur. Ceram. Soc. 41[15] (2021) 7886-7892.
24. J. Song, G. Lee, J. Kim, and J. Lee, Ceram. Process Res. 19[4] (2018) 279-284.
25. S. Chen, Journal of National Museum of China. 9 (2011) 147-152.
26. L. Wang, H. Duan, J. Zhu, Y. Yan, Y. Xie, and C. Wang, Nuclear Techniques. 33[4] (2010) 246-252.
27. L. Wang, J. Zhu, C. Wang, Y. Yan, H. Duan, and Y. Xie, in Proceedings of Academic Seminar on Chinese Red and Green Color Porcelain, July 2011, edited by X. Guo (Cultural Relics Press, 2011) p. 249.
28. P. Colomban, F. Ambrosi, A. Ngo, T. Lu, X. Feng, S. Chen, and C. Choi, Ceram. Int. 43[16] (2017) 14244-14256.
29. J. Pevenage, D. Lauwers, D. Herremans, E. Verhaeven,

B. Vekemans, W. Clercq, L. Vincze, L. Moens, and P. Vandenabeele, Anal. Methods-UK. 6 (2014) 387-394.
30. M. Hidaka, K. Ohashi, S. Kajihara, R.P. Wijesundera, L.S.R. Kumara, J.-Y. Choi, and N.E. Sung, Ceram. Int. 35[2] (2009) 875-886.
31. W. Hao, W. Luo, Y. Chen, and C. Wang, J. Raman Spectrosc. 45[3] (2014) 224-227.
32. Q. Pan, J. Shao, R. Li, L. Cheng, and R. Wang, Spectrosc. Spect. Anal. 42[3] (2022) 732-736.
33. M. Marco de Lucas, F. Moncada, and J. Rosen, J. Raman Spectrosc. 37 (2006) 1154-1159.
34. R. Van Grieken and A. Markowicz, in "Handbook of X-ray Spectrometry" (CRC Press, 2002) p. 407.
35. D. Faria and F. Lopes, Vib Spectrosc. 45 (2007) 117-121.
36. T. Zhang, in "Ming History-Volume 67" (Zhonghua ShuJu, 1974).
37. X. Liu, in Proceedings of the Exhibition of Yongle Xuande Kiln Porcelain Unearthed at Zhushan, 1989, edited by Hong Kong Museum of Art (Hong Kong Urban Council Press, 1989) p. 12-53.
38. Z. Huang, in "Ming shilu-Yingzong shilu Forty seven" (Institute of Historical and Linguistic Research, Academia Sinica, 1962) p.77.
39. Y. Sun, Antiquity. 09 (1959) p. 29-31.
40. Z. Gong, in "Jingdezhen Pottery Song" (Zhonghua ShuJu, 1912-1948) p. 5.
41. Y. Zhu, in "Tao Shuo" (Zhonghua ShuJu, 1914) p. 28.
42. D. Zhang, in "The Night Boat" (Zhejiang Ancient Books Press, 2012) p. 498.
43. Y. Zhu, in "Tao Shuo- Volume 1" (Zhonghua ShuJu, 1914) p. 205.
44. Z. Huang, in "Ming shilu-Xiaozong shilu Fifteen" (Institute of Historical and Linguistic Research, Academia Sinica, 1962) p. 43.
45. Z. Huang, in "Ming shilu-Xiaozong shilu Nineteen" (Institute of Historical and Linguistic Research, Academia Sinica, 1962) p. 32.
46. Z. Huang, in "Ming shilu-Xiaozong shilu Thirty nine" (Institute of Historical and Linguistic Research, Academia Sinica, 1962) p. 8.
47. F. Xu, in "Da Ming Huidian- Volume 201" (Jiangsu Guangling Ancient Books Press, 1989) p. 5987.
48. Y. Huang, in "Things Cyanote" (Qilu Press, 1591) p. 398.
49. X. Feng, Z. An, Q. An, B. Zhu, Q. Wang, in "A History of Chinese Ceramics" (Antiquity Press, 1982) p. 384.
50. L. Wang, J. Zhu, W. Gao, S. Tian, Y. Xie, S. Chu, Y. Yan, and C. Wang, in Proceedings of Shanxi University 2008 National Doctoral Academic Forum, Sep. 2008, p. 1152-1160.
51. M. Bouchard and D.C. Smith, Spectrochim. Acta. A. 59[10] (2003) 2247-2266.
52. L. Wang, J. Zhu, Y. Yan, Y. Xie, and C. Wang, J. Raman Spectrosc. 40[8] (2009) 998-1003.
53. F. Perez-Robles, F.J. Garcia-Rodriguez, S. Jimenez-Sandoval, et al., J. Raman Spectrosc. 30[12] (1999) 1099-1104.
54. L. Wang, J. Zhu, W. Gao, S. Tian, Y. Xie, S. Chu, Y. Yan, and C. Wang, in Proceedings of Shanxi University 2008 National Doctoral Academic Forum, Sep. 2008, p. 1152-1160.
55. D.L.A. de Faria, S. Venancio Silva, and M.T. de Oliveira, J. Raman Spectrosc. 28[11] (1997) 873-878.
56. D. Bersani, P.P. Lottici, and A. Montenero, J. Raman Spectrosc. 30[5] (1999) 355-360.
57. Z. Cvejic, S. Rakic, A. Kremenovic, B. Antic, C. Jovalekic, and P. Colomban, Solid State Sci. 8[8] (2006) 908-915.
58. D. Neff, S. Reguer, L. Bellot-Gurlet, Ph. Dillmann, and R. Bertholon, J. Raman Spectrosc. 35[8] (2004) 739-745.
59. E. Owens and J. Orosz, Solid State Commun. 138[2] (2006) 95-98.
60. P. Xu, R. Li, in "Raman Spectroscopy in Geology" (Xi'an: Shanxi Science and Technology Press, 1996) p. 46-51.
61. J. You, G. Jiang, H. Hou, H. Chen, Y. Wu, and K. Xu, J. Raman Spectrosc. 36[3] (2004) 237-249.
62. F. Froment, A. Tournié, and P. Colomban, J. Raman Spectrosc. 39[5] (2008) 560-568.
63. Ph. Colomban. J. Cult. Herit. 9 (2008) e55-e60.
64. A. Zoppi, C. Lofrumento, E. Castellucci, C. Dejoie, and Ph. Sciau, J. Raman Spectrosc. 37[10] (2006) 1131-1138.
65. A. Zoppi, C. Lofrumento, E.M. Castellucci, C. Dejoie, and Ph. Sciau, J. Raman Spectrosc. 39[1] (2008) 40-46.
66. W. Hao, W. Luo, Y. Chen, and C. Wang, J. Raman Spectrosc. 45[3] (2014) 224-227.
67. Q. Li, A. Wu, M. Zhang, J. Li, J. Cao, H. Li, and Y. Jiang, Materials. 17 (2024) 2800.
68. Ministry of Commerce, People's Republic of China, in "Technical Guide for Export Commodities-Daily Use Ceramics" (Commercial Press, 2005) p. 1.